

Surfactant Chain Length Effects on Nanoparticles of Biodegradable Polymers for Targeted Drug Delivery

Yutao Liu

Dept. of Chemical & Biomolecular Engineering, National University of Singapore, 4 Engineering Drive 4, Singapore 117576, Singapore

Si-Shen Feng

Dept. of Chemical & Biomolecular Engineering, National University of Singapore, 4 Engineering Drive 4, Singapore 117576, Singapore

Dept. of Bioengineering, National University of Singapore, 9 Engineering Drive 1, Singapore 117576, Singapore

Nanoscience and Nanoengineering Initiative (NUSNNI), National University of Singapore, 2 Engineering Drive 3, Singapore 117581, Singapore

DOI 10.1002/aic.13728

Published online January 17, 2012 in Wiley Online Library (wileyonlinelibrary.com).

Folic acid-conjugated nanoparticles (NPs) of biodegradable polymer poly(lactic-co-glycolic acid) (PLGA), which were emulsified by long-chain D- α -tocopheryl polyethylene glycol succinate (vitamin E TPGS or simply TPGS) for targeted delivery of anticancer drugs, are prepared. The NPs were characterized for their size and size distribution, surface morphology, surface charge, drug encapsulation efficiency, and surface chemistry. The cellular uptake and the cytotoxicity of the drug-loaded PLGA NPs were assessed in vitro with MCF7 breast cancer cells in close comparison with the corresponding Short-chain TPGS (TPGS2k)-coated PLGA NPs and the original drug. The long-chain TPGS 2000 (TPGS2k)-emulsified PLGA NPs showed great advantages over the short-chain TPGS 1000 (TPGS1k)-emulsified and the nude PLGA NPs. The folic acid-conjugated TPGS2k-emulsified PLGA NPs showed significant advantages in cellular uptake and therapeutic effects in vitro. The IC₅₀ value showed 90.4% less than that of the original drug. © 2012 American Institute of Chemical Engineers AICHE J, 58: 3289–3297, 2012

Keywords: biodegradable polymers, cancer nanotechnology, chemotherapeutic engineering, drug delivery, drug targeting, nanoparticles

Introduction

Cancer is one of the most dread diseases today.¹ One in four deaths in the United States is due to cancer, although the combined death rate decreased by 21.0% for men between 1990 and 2006 and 12.3% for women between 1991 and 2006.² Nevertheless, the major cancer treatment in current regimen is still surgery followed by chemotherapy and/or radiotherapy, which are not satisfactory enough to suppress the disease. Despite serious side effects, chemotherapy still plays a major role in fighting against cancer due to its systemic property, which is a complicated procedure with a high risk. The side effects may come from the drug itself, its dosage form due to the adjuvant toxicity, restricted pharmacokinetics, and pharmacodynamics. Chemotherapeutic engineering may provide an ideal solution for those problems, which was defined as application and further development of

engineering especially chemical engineering principles to solve the problems in the current regimen of chemotherapy to achieve best efficacy with least side effects.^{3,4}

As a major technology in chemotherapeutic engineering, nanoparticle (NP) technology has been regarded as one of the most promising approaches to deal with cancer and has been extensively exploited to improve conventional chemotherapy in the recent years.^{5–9} Among various types of drug delivery systems in nanoscale, NPs of biodegradable polymers have been under intensive investigation and proof-of-concept experimental results have been achieved. It has been demonstrated for the first time in the literature that one 10 mg/kg dose of paclitaxel formulated in the poly(lactide-co-glycolide) (PLGA) NPs could realize 168-h effective chemotherapy in comparison with only 22-h treatment for Taxol[®] and the drug tolerance can be 400% higher with 3.6 times area-under-the-curve (AUC), a quantitative measurement of *in vivo* therapeutic effect.⁸ Such positive result was then confirmed by docetaxel, a better derivative of paclitaxel, formulated in the Poly(lactic acid)-D- α -tocopheryl polyethylene glycol succinate (PLA-TPGS) NPs. One 10 mg/kg dose of such a NP formulation realized 336-h effective

This article is published as a tribute to Professor Shu Chien, a pioneer of Bioengineering and a founder of Chemotherapeutic Engineering, for his 80th birthday anniversary on August 6, 2011.

Correspondence concerning this article should be addressed to S.-S. Feng at cheffss@nus.edu.sg.

chemotherapy in comparison with 24-h treatment for Taxotere[®]. The AUC was found to be 8.1 times larger for the former than that for the latter.⁹ These results relieved a major concern on chemotherapeutic engineering, for example feasibility—could the NPs escape from the recognition and elimination by the reticuloendothelial system (RES) to deliver the drug into the cancer cells? Another concern is the safety—how long the NPs would stay in the body and what the impact to health could be. This is a serious question we have to pursue, which has become an important branch in chemotherapeutic engineering (or cancer nanotechnology and nanomedicine). The advantages of the NP formulations over the traditional chemotherapy in current regimen may be due to their unique properties such as the small size, favorite surface chemistry, high drug encapsulation efficiency especially for hydrophobic drugs, controlled and sustained drug release manner, high cellular uptake efficiency, desired pharmacokinetics, long circulation half-life, and other highly tailored functions such as passive as well as active targeting.^{10–12} Furthermore, with further development, chemotherapeutic engineering may promote personalized chemotherapy; delivery of therapeutic agents across physiological drug barriers; and eventually, chemotherapy at home.¹³

NPs should be appropriately engineered before taking effect in practical cancer chemotherapy. There are several fundamental problems and technical barriers that must be overcome for anticancer drug delivery,¹⁴ which include opsonization and phagocytosis of NPs,¹⁵ capture and retention of NPs in RES,¹⁶ difficulties in NP accumulation near solid tumors and targeting the cancerous cells followed by penetration into solid tumors.^{17,18} The effective solution is to engineer NPs by tuning their size, polydispersity, surface area, surface charge, surface morphology as well as surface chemistry through introducing versatile surfactants to coat the NPs to enhance the drug delivery to the cancer cells, avoid being recognized by the macrophages and cross the various physiological drug barriers.

TPGS surfactants are amphiphilic macromolecules consisting of a hydrophilic polar polyethylene glycol (PEG) segment and a hydrophobic tocopheryl (vitamin E) segment.¹⁹ The TPGS that has been used for NPs formulation for drug delivery is TPGS 1000 (TPGS1k), which has been proved to be an effective surfactant for NP formation for drug delivery, for example, the quantity of TPGS needed to make the same amount of NPs is only 1/67 of poly(vinyl alcohol) (PVA) by weight.²⁰ Moreover, because of its bulky lipophilic segment, TPGS was thought to possess properties such as better drug solubilization, high emulsification effect, high drug encapsulation efficiency, high cellular adhesion, and adsorption.^{21–23} TPGS was also proved to be able to effectively block P-glycoprotein (P-gp) efflux pump which is a major component in the multidrug resistance system expressed on a lot of cancerous cells that removes the drug molecules from the cancerous cells, thus, alleviating bioavailability of the drug.^{24,25} Inhibition of P-gp allows drugs to be retained within the pathological cells enabling drug concentration to keep effective doses to kill the cells. Conversely, the PEG chains conjugated on TPGS1k could make NPs avoid opsonization and internalization by RES due to the PEGylation, which reduces the proteins to bind on the NPs.^{26–28}

In the literature, the PEG chain of the TPGS used for NP preparation so far is PEG 1000 (Mw = 1000). We denote the TPGS of PEG 1000 chain as TPGS1k. Nevertheless, the

chain length of PEG in TPGS macromolecules are adjustable and PEG 1000 might not be long enough to fulfill the requirement to make stealth NPs to avoid RES scavenging and protein adsorption, which could lowering the circulation life time of the NPs in bloodstream because it is believed that only molecular weight of PEG not shorter than 2000 should be required to achieve those benefits.^{15,29} In 2006, researchers synthesized a series of TPGS analogs with a variety of PEG chain length and indicated that the transportation of rhodamine 123 in Caco-2 cells was influenced by the chain length of PEG.³⁰ It is thus inspired that the performance of the TPGS-emulsified NPs may be dependent on its PEG chain length, which may be a decisive factor that has been ignored in the literature of NPs for drug delivery. Therefore, we conducted a systematic research on the possible effects of the PEG chain length in the surfactant TPGS.

In this work, we synthesized a series of TPGS_nk surfactants of various PEG chain lengths to demonstrate the effectiveness of those enhanced surfactants in the NPs formation for targeted drug delivery with docetaxel as a model anticancer drug, which is one of the best antineoplastic agents against a wide spectrum of cancers.³¹ It is expected that the TPGS of optimal PEG chain length could be found for best performance of the NPs for targeted drug delivery. Folic acid-functionalized TPGS was also synthesized to provide the possibility of active targeting to the cancer cells of folate receptors (FRs) overexpression. The effects of the surfactant chain length on the physicochemical and pharmaceutical properties and *in vitro* cellular uptake and cytotoxicity of the PLGA NPs prepared by the nanoprecipitation method were investigated. Such a chemotherapeutic engineering technology devoids of toxic additives such as PVA. Although *in vitro*, our results showed that TPGS_nk, especially TPGS2k has great advantages in NPs formulation for drug delivery over the commercial formulation of docetaxel, Taxotere[®] and supplies more choices for engineering versatile polymeric NPs by selecting among the surfactants of different chain length in the family.

Experimental

Materials

Docetaxel (anhydrous, 99.56%) was purchased from Shanghai Jinhe Bio-Technology, China. Taxotere[®] was provided by National Cancer Center (Singapore). TPGS1k, poly[D,L-lactide-*co*-glycolide] (PLGA, 75:25, Mw = 90,000–126,000), monomethoxy PEG (MPEG, Mw = 2000 and 5000, from now on simply MPEG2k and MPEG5k, respectively), tocopheryl succinate (or vitamin E succinate, VES), dicyclohexylcarbodiimide (DCC), 4-(dimethylamino) pyridine (DMAP), *N*-hydroxysuccinimide (NHS), triethylamine (TEA), *N*-(3-Dimethylaminopropyl)-*N'*-ethylcarbodiimide hydrochloride (EDAC), folic acid, sucrose, methanol, ethanol, dichloromethane (DCM), diethyl ether, acetone, acetonitrile (ACN), dimethyl sulfoxide (DMSO), coumarin-6, phosphate-buffered saline (PBS, pH 7.4), 3-(4,5-dimethylthiazol-2-yl)-2,5-diphenyl tetrazolium bromide (MTT) assay, and propidium iodide (PI) were purchased from Sigma-Aldrich (St. Louise, MO). Poly[ethylene glycol]-2000 bis-amine (PEG2k bis-amine) was offered by Laysan Bio (Arab, AL). Tween-80 was from ICN Biomedicals (OH). Triton X-100 was provided by USB Corporation (OH). Fetal bovine serum (FBS), trypsin-EDTA solution, and penicillin-streptomycin solution were purchased from Invitrogen. Dulbecco's modified Eagle's medium (DMEM)

was from Sigma. All solvents used in this study were high-performance liquid chromatography (HPLC) grade. MCF7 breast cancer cells were provided by American Type Culture Collection (ATCC). The water used was pretreated with the Milli-Q® Plus System (Millipore Corporation, Bedford).

Synthesis of TPGS n k surfactants

The surfactants of TPGS n k ($n = 2$ or 5) were synthesized by carbodiimide chemistry. Briefly, tocopheryl succinate was weighed and dissolved in DCM. MPEG2k or MPEG5k was also weighed and dissolved in DCM. Both the tocopheryl succinate and MPEG were then added together with DCC and DMAP with stoichiometric ratio of 1:1.2:0.1, respectively, and left to stir overnight in nitrogen environment at dark. The solution was then filtered to remove byproduct and precipitated in cold diethyl ether. The precipitate obtained was then washed by diethyl ether again and dissolved in water and dialyzed against water. The milky dispersion was filtered again to remove impurities and the filtrate was collected. TPGS 2000 (TPGS2k) and TPGS 5000 (TPGS5k) powder were obtained after freeze drying of the filtrate. For amine-terminated TPGS, tocopheryl succinate, PEG2k bis-amine, DCC, and NHS were weighed and dissolved in DCM separately with stoichiometric ratio of 1:1.2:2:2, respectively. The solution was mixed with 20 μ l of TEA and left to stir in nitrogen environment at dark for 2 days. The solution was then filtered to remove byproduct and precipitated in cold diethyl ether. The precipitate obtained was then washed by diethyl ether again and dissolved in water and dialyzed against water. The milky dispersion was filtered again to remove impurities and the filtrate was collected. D- α -Tocopheryl amino polyethylene glycol 2000 succinate (TPGS2kNH₂) powder was obtained after freeze drying the filtrate. The ¹H NMR spectra were collected on a Bruker ACF300 (300 MHz) spectrometer using *d*₆-DMSO as solvent.

Preparation of PLGA NPs

NPs were prepared by the nanoprecipitation method. The aqueous phase was first prepared by dispersing the TPGS n k surfactants in ultrapure water at concentration of 0.08 mg/ml. PLGA was weighed and dissolved in acetone forming a 10 mg/ml oil phase. The oil phase was then added dropwise into 10 times of the aqueous phase while continuously stirring. The particle suspension was left to stir until all the solvent was evaporated. The particle suspension was then filtered and centrifuged and washed three times at 8000 rpm for 15 min at 4°C. The powder of the NPs was obtained after freeze drying. The docetaxel loaded NPs were fabricated using the same method with the 5% (w/w) drug-contained oil phase. The fluorescent NPs were fabricated by the same procedure except for 0.5% (w/w) coumarin-6-contained oil phase. Formulations without surfactant added in the process were prepared using the same method but replacing the aqueous phase with only ultrapure water. From now on, PLGA NP, T1k NP, T2k NP, and T5k NP are assigned in abbreviation to the NPs with no surfactant, TPGS1k, TPGS2k, and TPGS5k used as surfactant, respectively.

Conjugation of folic acid onto the TPGS2kNH₂-coated NPs

Postconjugation strategy (i.e. conjugation of ligand onto the NPs surface instead of conjugation of ligand onto the polymer before NPs formulation) to link the folic acid to the

TPGS2kNH₂-coated NPs was applied. Suspended NPs were mixed with folic acid at a molar ratio of 20:1. *N*-(3-Dimethylaminopropyl)-*N'*-ethylcarbodiimide hydrochloride (EDAc) and NHS were added in excess and the suspension was stirred overnight before filtering through a filter paper. Filtrate collected was dispersed in ultrapure water and washed three times. The particles were collected and freeze dried. Similarly, T2kN NP and T2k NP-FOL infer TPGS2kNH₂-coated NPs and the NPs coated by TPGS2kNH₂ and further conjugated by folic acid, respectively.

Characterization of the NPs

The average particle size and size distribution of the NPs were measured using laser light scattering (LLS, 90Plus Particle Sizer, Brookhaven Instruments Corporation, Huntsville, NY) at a laser angle of 90° at 25°C. The sample was prepared by diluting the NP suspension with ultrapure water and sonicating for 1 min to ensure homogenous dispersion of the particles. The surface charge of the NPs in water was measured using a zeta-potential analyzer (Zeta Plus, Brookhaven Instruments Corporation) at 25°C. The sample was prepared by diluting the NP suspension with ultrapure water and sonicating for 1 min to ensure homogenous dispersion of the particles. The zeta-potential was measured under certain pH value and concentration of the dispersion. The drug loading efficiency of the NPs was determined in triplicates by HPLC (Agilent LC 1100 series). A reversed phase Inertsil® ODS-3 column (250 \times 4.6 mm, particle size 5 μ m; GL Science, Tokyo, Japan) was used. Three milliliters of NP suspension with known amount of NPs was freeze dried, redissolved in 1 ml of DCM, and left overnight to evaporate. Four milliliters of mobile phase (50:50, v/v ACN/water solution) was added and the solution was filtered using a 0.45 μ m poly(vinylidene fluoride) (PVDF) syringe filter before being transferred to a HPLC vial. The effluent was detected at 230 nm with a UV-VIS detector. Comparison between the AUC readings obtained from the sample to previously prepared calibration curve yielded the amount of docetaxel within the sample. The drug loading is defined as the ratio between the mass of drug encapsulated in the NPs and the mass of the NPs presented.

Surface morphology

The surface morphology of the NPs was visualized using field emission scanning electron microscope (FESEM, JSM-6700F, JEOL, Tokyo, Japan) at an accelerating voltage of 5 kV. The samples were prepared by placing a drop of the NP suspension on copper tape placed on top of a sample stub and left under reduced pressure to dry. The sample was then coated with a platinum layer using Auto Fine Coater (JEOL) for 30 s at 30 mA current.

Surface chemistry

The surface chemistry of the NPs was assessed using x-ray photoelectron spectroscopy (XPS, AXIS His-165 Ultra, Kratos Analytical, Shimadzu Corporation, Japan). The samples were analyzed using a fixed transmission mode covering a range of binding energy from 0 to 1100 eV with pass energy of 80 eV. Peak curve fitting was performed using software provided by the instrument manufacturer.

In vitro cellular uptake of the NPs

Cell line experiments were carried out using human breast adenocarcinoma (MCF7) cells cultured in DMEM

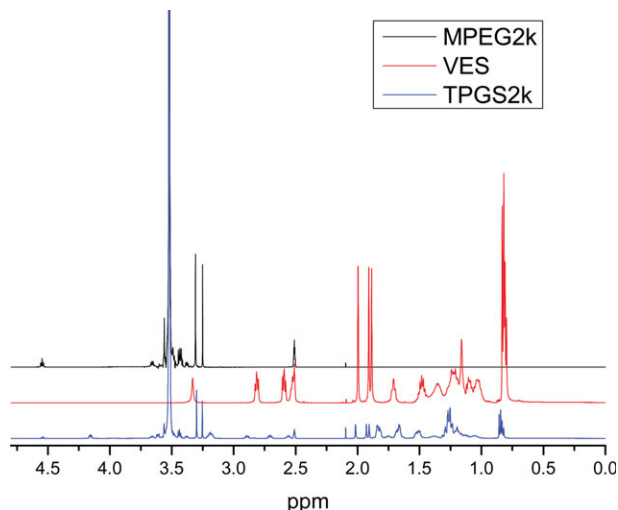


Figure 1. ^1H NMR spectra of MPEG2k, VES, and TPGS2k.

[Color figure can be viewed in the online issue, which is available at wileyonlinelibrary.com.]

supplemented with 10% FBS and 1% penicillin–streptomycin as the antibiotics in humidified environment of 5% CO_2 at 37°C . Growth medium was replenished every other day and subculture was performed when cells reached 80% confluence.

For quantitative study, MCF7 cells were seeded into 96-well black plates (Costar, IL,) at 5×10^3 cells/well (0.1 ml) and after the cells reached 80% confluence, the medium was changed to the suspension of coumarin-6 loaded NPs at a NP concentration of 0.125 mg/ml for 2 h. After incubation, the NP suspension in the testing wells was removed and the wells were washed with 0.1 ml PBS three times to remove the NPs outside the cells. After that, 50 μl of 0.5% Triton X-100 in 0.2 N NaOH solution was added to lyse the cells. The fluorescence intensity present in each well was then measured by microplate reader (Genios, Tecan, Switzerland) with excitation wavelength at 430 nm and emission wavelength at 485 nm.

For qualitative studies, MCF7 cells were seeded in a chambered cover glass system (LAB-TEK[®], Nalgene International, Naperville, IL) in humidified environment of 5% CO_2 at 37°C . After incubation of 24 h, the medium was replaced by coumarin-6-loaded NP suspension at a concentration of 0.125 mg/ml. Cells were incubated again for 2 h and washed thrice with PBS. Cells were then fixated by addition of 75% ethanol for 20 min. Cells were further washed twice with PBS and nuclei counterstaining was carried out with PI for 45 min. The cells were washed twice with PBS. Finally, the cells were observed using confocal laser scanning microscope (CLSM, Olympus Fluoview FV1000) using a PI and FITC channel.

In vitro cytotoxicity

MCF7 cells were seeded in 96-well transparent plates (Costar, IL) at 5×10^3 cells/well (0.1 ml) and after 12 h, the old medium was removed and the cells were incubated for 24, 48, and 72 h in the medium containing Taxotere[®] or docetaxel loaded NP suspension at an equivalent drug concentration of 0.5, 0.25, 0.1, and 0.025 $\mu\text{g}/\text{ml}$. The NPs were sterilized with UV irradiation for 1 day before use. At given time intervals, the cultured cells were assayed for cell viability

with MTT. The wells were washed twice with PBS and 10 μl of MTT supplemented with 90 μl culture medium was added. After 3 h incubation, the medium was removed and the precipitate was dissolved in DMSO. The absorbance of the wells was measured by the microplate reader (Genios) with wavelength at 570 nm and reference wavelength at 620 nm. Cell viability was calculated by the following equation: $\text{cell viability} = \text{Abs}_s / \text{Abs}_{\text{control}} \times 100\%$, where Abs_s is the absorbance of the wells containing the cells incubated with the NP suspension and $\text{Abs}_{\text{control}}$ is the absorbance of the wells containing the cells incubated with the culture medium only (positive control).

Statistical analysis

Data were expressed as the means with 95% confidence intervals. Statistical tests were performed with the Student's *t* test. For all tests, *P* values less than 0.05 were considered to be statistically significant. All statistical tests were two tailed.

Results and Discussion

Synthesis of various surfactants

TPGS n k ($n = 2$ and 5) surfactants were synthesized using the carbodiimide reaction. ^1H NMR was applied to confirm the successful conjugation of PEG n k molecules with VES. Typically, the results of TPGS2k from the NMR analysis are shown in the Figure 1. This figure shows a comparison among MPEG2k, VES, and TPGS2k. Most peaks that occur in the spectrum of MPEG2k and VES also occur in the spectrum of TPGS2k, albeit slightly shifted, showing a strong resemblance between the structures of the basic compounds and the product as well as the change of chemical environment in the product. With the results, it can be said that TPGS2k has been successfully synthesized. TPGS5k was synthesized similarly except MPEG5k instead of MPEG2k was used. The other functionalized material, TPGS2kNH₂ was also synthesized using the carbodiimide reaction in the presence of NHS. The reaction resulted in the formation of yellowish solid. Figure 2 shows a comparison among PEG2k bis-amine, VES, and TPGS2kNH₂. All peaks that occur in

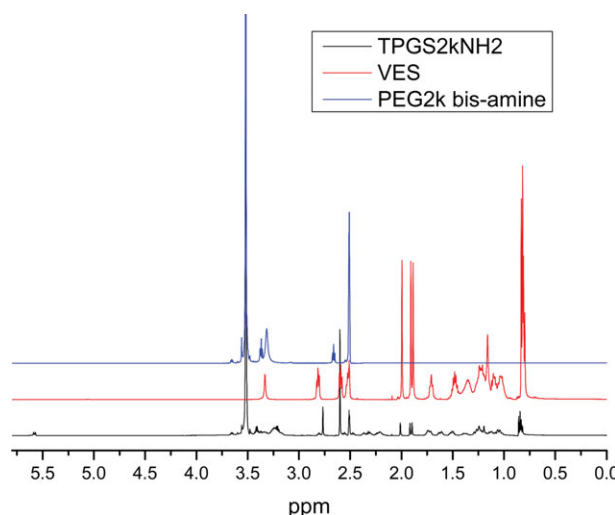


Figure 2. ^1H NMR spectra of PEG2k bis-amine, VES, and TPGS2kNH₂.

[Color figure can be viewed in the online issue, which is available at wileyonlinelibrary.com.]

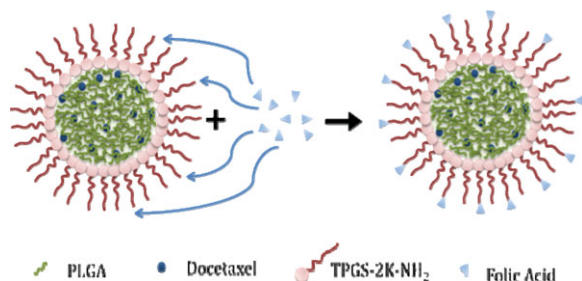


Figure 3. Schematic illustration of the structure of the nanoparticles and the postconjugation of folic acid onto the particles.

[Color figure can be viewed in the online issue, which is available at wileyonlinelibrary.com.]

the spectrum of PEG and VES also occur in the spectrum of TPGS2kNH₂ with slight shift, pointing to a successful synthesis of TPGS2kNH₂.

Preparation of NPs

The NPs were prepared by the nanoprecipitation method, which requires two miscible solvents with the first solvent (acetone) dissolving the drug and polymer and the second solvent (water) dispersing the surfactant. The drug and polymer should not be dissolved in the second solvent. The addition of the polymer-containing solvent into the dispersing medium causes a rapid desolvation of the polymer and formation of drug-entrapped NPs.³² The surfactants dispersed in aqueous phase were subsequently adsorbed onto the surface of the NPs due to hydrophobic interaction. Surface coating of NPs was thus achieved by the various desired surfactants. The factors taken into account during the fabrication include the type of organic solvent, the surfactant to solvent ratio, the rate of addition of polymer solution, and temperature. Several batches of PLGA NPs without drug, with docetaxel or coumarin-6 loaded were successfully fabricated. The surfactants used during the fabrication included TPGS1k, TPGS2k, and TPGS5k. TPGS1k is a commercial product, which was used as a comparison to benchmark the effectiveness of the newly synthesized surfactants in this work.

Conjugation of folic acid to the NPs

The conjugation of folic acid onto the NPs was proposed to fulfill the targeted delivery purpose aiming to target the cancerous cells, which are of FRs overexpression. Ligand conjugation can be made in two ways in the literature: post-conjugation means that the ligand conjugation is made after the NPs formulation and preconjugation means that conjugating the ligand to the polymer first and the NPs are then formulated. The former one was used in this work that was achieved via the aqueous phase carbodiimide reaction between folic acid and the free amine groups on

TPGS2kNH₂-coated NPs using EDAc and NHS. The schematic diagram of the structure of the NPs and the reaction is illustrated in Figure 3. The merit of postconjugation for attaching the targeting ligands onto NPs is that it ensures the ligands to stay on the top of the particles but not buried inside the spheres.

Characterization of the NPs

Particle Size and Size Distribution. The size of the NPs plays an important role in determining their performance in chemotherapy. Smaller size NPs may be able to permeate more easily through the biological barriers and penetrate the epithelial cells via endocytosis. However, too small NPs may not have enough surface energy to overcome the bending energy needed in the endocytosis process. Moreover, too small NPs may be resulted in too low drug encapsulation efficiency and too fast drug release kinetics. The ability of the NP to target and accumulate in cancer cells is also affected by its size. The size and size distribution of the NPs with different surfactants are compared in Table 1. From Table 1, the NP size measured using LLS is between 200 and 250 nm. The optimal range of NPs for cellular uptake by endocytosis was found to be 100–200 nm in our earlier publications.³³ The size of the NPs coated by the long-chain TPGS2k and TPGS5k falls in or near this optimal range. The NPs conjugated with folic acid are slightly larger in size due to the extra folic acid tail attached to the surface. The size distribution is quite narrow indicating that the NPs are quite uniform in size. Narrow size distribution would allow for better control of the properties of the NPs.

Surface charge

The surface charge of the folic acid-conjugated, drug-loaded PLGA NPs was measured by the zeta-potential analyzer, which indicates the stability of the particle dispersion. Surface charge that is highly negative or positive points to a stable colloidal suspension due to the high repulsion force between the NPs. NPs with low colloidal stability tend to aggregate and form large aggregates, losing some of the properties in the nanoscale. In addition, NPs that are very negative are believed to be hindered from crossing the cell membrane due to the negative nature of the cell membrane, which might repel the NPs. All the NPs prepared in this work have negative surface charges below -19 mV.

Drug loading

Drug loading is defined as the amount (weight) of drug encapsulated in the NPs of a given weight, which is represented by the units of μg drug per mg NPs. The results are summarized in Table 1. The drug loading of T2k NP is the highest in comparison to other NP formulations. This suggests that TPGS2k is more effective than other conventionally used surfactants in ensuring that more drugs were

Table 1. Characteristics of the Docetaxel-Loaded PLGA NPs with Various Surfactants TPGS_nk: Particle Size, Size Distribution, Zeta-Potential, and Encapsulation Efficiency

Nanoparticles	Particle Size (nm)	Polydispersity	Zeta-Potential (mV)	Drug Loading ($\mu\text{g}/\text{mg}$ NP)
NP	206.7 ± 2.9	0.065 ± 0.027	-42.57 ± 0.60	8.23 ± 0.026
T1k NP	215.8 ± 2.7	0.035 ± 0.014	-21.48 ± 1.14	5.60 ± 0.040
T2k NP	202.3 ± 6.1	0.069 ± 0.049	-22.21 ± 0.98	28.48 ± 0.110
T5k NP	249.2 ± 16.6	0.225 ± 0.028	-24.91 ± 0.80	36.90 ± 4.170
T2k NP-FOL	241.5 ± 4.3	0.150 ± 0.023	-19.00 ± 0.82	3.79 ± 0.054

Data represent mean \pm SE, sample # 3.

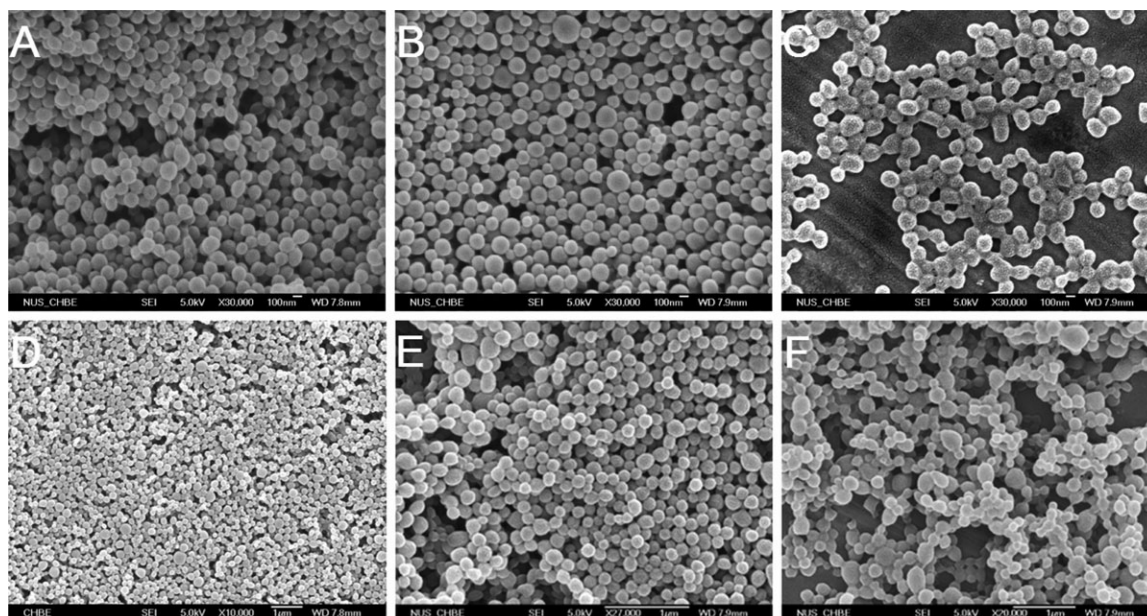


Figure 4. FESEM images of (A) PLGA NP, (B) T1k NP, (C) T2k NP, (D) T5k NP, (E) T2kN NP, and (F) T2k NP-FOL.

entrapped within PLGA matrix. The higher drug loading also hint at the potential of TPGS2k to be used as a surfactant to produce NPs that are effective drug carriers with appropriate size and stability.

Particle morphology

High-resolution images to study the surface morphology of the NPs were obtained using FESEM (Figure 4). Particles of different formulations were shown to be about 200–250 nm, consistent with the results obtained from LLS. In addition, the particles were revealed to be generally spherical in shape and uniform in size. The NPs prepared using different surfactants were quite similar in visualization. The surface of the NPs was also revealed to be smooth on the images.

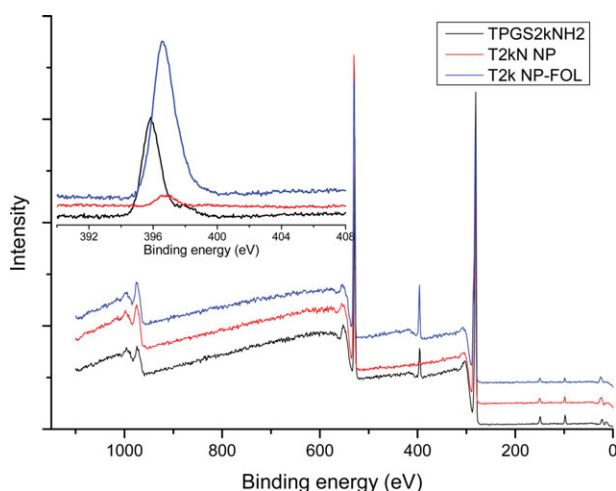


Figure 5. XPS wide-scan spectra of the synthesized product TPGS2kNH₂ (lower curve), T2kN NP (middle curve), and T2k NP-FOL (upper curve).

The inset graph shows the N 1s spectra of those three with the same sequence. [Color figure can be viewed in the online issue, which is available at wileyonlinelibrary.com.]

However, T2k NP-FOL formulation was seen to be more adhesive than others, which could be attributed to the bulky condition of the surface causing entanglement between particles after drying.

Surface chemistry

To confirm the existence of the primary amine groups as well as the folic acid on the NPs' surface, surface chemical composition of the NPs was elucidated from the specific binding energy on the XPS spectrum. Figure 5 shows the wide scan and comparison among TPGS2kNH₂, T2kN NP, and T2k NP-FOL. To prove the successful synthesis of TPGS2kNH₂, nitrogen was specifically scanned. From the inset of Figure 5, a peak for nitrogen at a binding energy of 396 eV was observed in the XPS spectrum, indicating the successful conjugation of amino PEG onto VES resulting in the product. In addition, the nitrogen peak can be observed in the spectrum of both the T2kN NP and T2k NP-FOL, demonstrating the presence of the surfactant on the surface of the NPs. The slight shift of the position of the nitrogen peak from the two NPs is possibly due to the change of the chemical environment near the surfactants, that is the presence of PLGA. The signal due to nitrogen on T2k NP-FOL was higher can be assigned to the presence of more nitrogen atoms in the chemical structure of folic acid (seven nitrogen atoms in one folic acid molecule).

In vitro cellular uptake of the NPs

The ability of the particles to penetrate into the cells and be internalized and retained within the cell is important to achieve the objective of delivering drugs. Targeting effects of folic acid conjugation can also be examined. The qualitative cellular uptake analysis was conducted by visualization of the internalized coumarin-6-loaded NPs using CLSM. Figure 6 shows the images of MCF7 human adenocarcinoma cells, which had internalized fluorescent loaded NPs. The images in rows A–E are of various NP formulations in the following order: NPs without surfactant, T1k NPs, T2k NPs, T5k NPs, and T2k NP-FOL. The images in column 1 were obtained using the FITC channel, which reveals the green

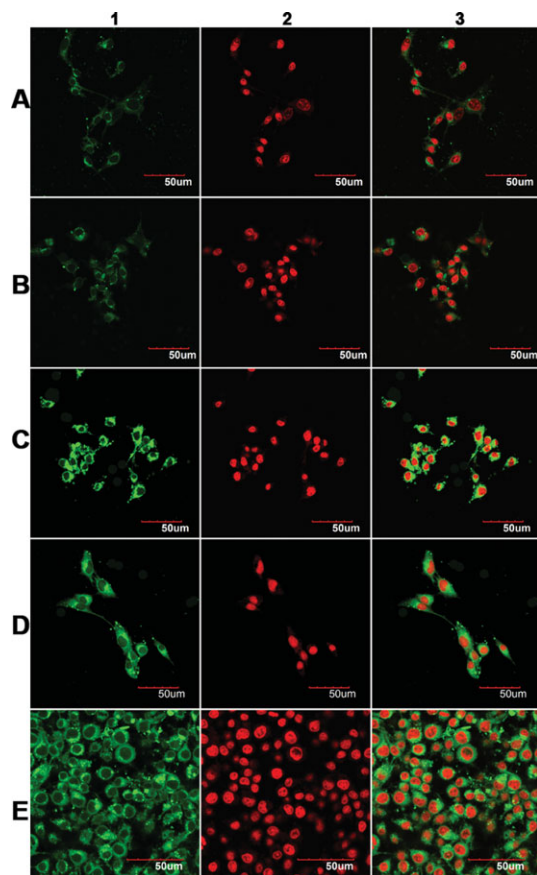


Figure 6. Confocal laser scanning microscope (CLSM) images of the particles internalized in MCF7 cells.

Rows A–E show PLGA NP, T1k NP, T2k NP, T5k NP, and T2k NP-FOL used, respectively. [Color figure can be viewed in the online issue, which is available at wileyonlinelibrary.com.]

fluorescence of coumarin-6-loaded NPs. Column 2 contains images obtained using the PI channel that highlights the nuclei stained by PI in red fluorescence. Column 3 lists the images that were overlaid by the FITC and PI channels. The images in column 3 shows the nucleus of the cells surrounded by green fluorescence from the coumarin-6-loaded NPs distributed in cytoplasm. The particles coated by the surfactant TPGS_{nk} were also successfully internalized with noticeably higher concentrations within the cells as can be seen from the brighter green fluorescence in the images. The comparison of the particles retained in the cells between folic acid-conjugated NPs (T2k NP-FOL) with nonligand attached NPs (T2k NP) demonstrated the FR-targeted behavior from the ligand-conjugated NPs. Folic acid and its conjugate were widely used for selective delivery of anticancer agents to cells with FRs. Folic acid is able to be efficiently internalized into the cells through the receptor-mediated endocytosis (RME). In the condition of the same exciting laser intensity from the same confocal microscope, after incubating 2 h, the fluorescence distribution of T2k NP-FOL in the cytoplasm (row E) is significantly higher than that of T2k NP (row C). It can be explained that RME facilitates and promotes the entry of the NPs into cells when the folic acid-conjugated NPs meet the overexpressed FRs on MCF7 cells.^{34,35} Apart from that, quantitative measurement also

evidently displayed the higher cellular uptake efficiency of folic acid-conjugated NPs. The efficiency for the T1k NP, T2k NP, T5k NP, and T2k NP-FOL is 42.8%, 14.3%, 23.1%, and 45.4% higher than that of the PLGA NPs, respectively (two-tailed Student's *t* test, $P < 0.05$). The finding supports the hypothesis that the new surfactant provides the opportunity to conjugate with folic acid for targeted delivery to specific cancerous cells.

In vitro cytotoxicity

The *in vitro* therapeutic efficacy of the drug delivery system was demonstrated in the cytotoxicity measurement (Figure 7). The cytotoxicity was measured by the cell viability: lower cell viability or survival rate would translate to higher cytotoxicity. A general decreasing cell viability trend was observed with increasing incubation times for the different formulations tested. Longer incubation time would mean

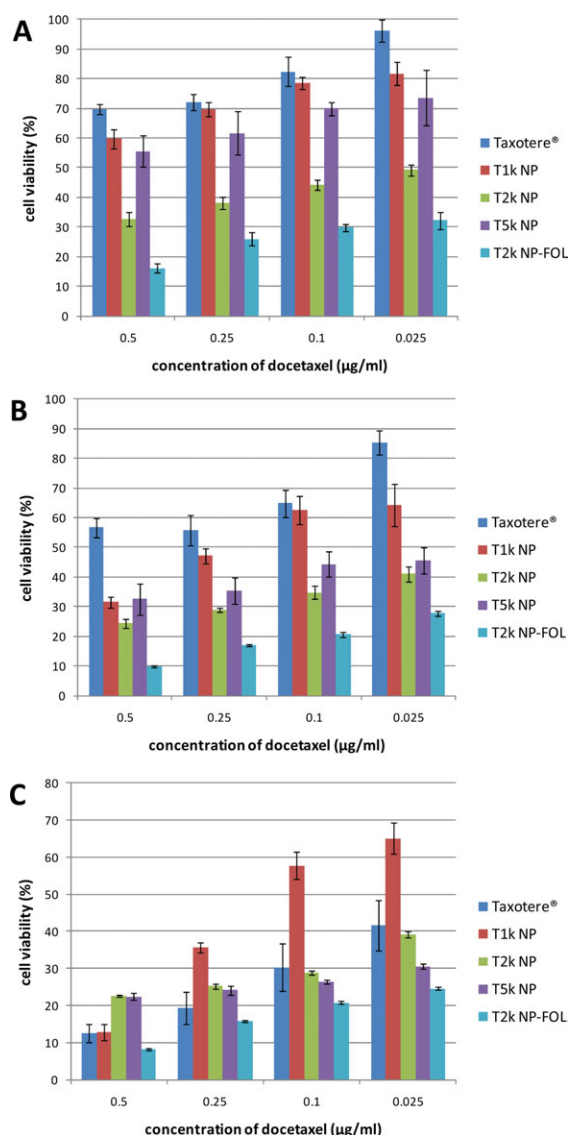


Figure 7. MCF7 cell viability measurement after 24 h (A), 48 h (B), and 72 h (C) treated by formulations of Taxotere®, T1k NP, T2k NP, T5k NP, and T2k NP-FOL at various drug concentrations.

[Color figure can be viewed in the online issue, which is available at wileyonlinelibrary.com.]

Table 2. IC₅₀ Values (μg/ml) of Various PLGA Nanoparticle Formulations of Docetaxel in the Various Designated Period of Cell Culture

	Taxotere [®]	T1k NP	T2k NP	T5k NP	T2k NP-FOL
24 h	0.98	2.13	0.026	1.44	0.0025
48 h	0.53	0.15	0.0068	0.014	0.0026
72 h	0.016	0.082	0.0041	7.17×10^{-5}	0.0023

longer exposure of the cells to the NPs carrying the drug, allowing more time for the NPs to internalize into the cells and release the loaded drugs in the cytoplasm, resulting in higher cell mortality. It was also observed that higher drug concentrations lead in lower cell viability, which is quite straightforward to understand. The highest cell mortality appeared at the highest concentration of the NP formulation after the longest treatment time suggesting that the drugs were released controllably and sustainably over a period of time, which is consistent with our previous study.⁸ From Figure 7, the cell viability from the groups treated by the various NP formulations were found to be generally lower than that treated by Taxotere[®], especially in the lower drug concentration groups, which infers the comparable and even better capability of the NP formulations to defeat cancer cells. When compared the viability results of the long-chain surfactant-coated NPs with those of TPGS (i.e. TPGS1k) surface coating, the performance of T2k NPs and T5k NPs was clearly better in general. It would be interesting to have a focused investigation on the possible impact of the various TPGS_{nk} surfactants on the drug release kinetics as it would demonstrate if there is any initial burst behavior and further reveal the reasons for the improved performance of the drug delivery system in cancer cell inhibition. We have had a plan to investigate *in vitro* drug release profiles as well as *in vivo* pharmacokinetics of those systems in our future studies.

In addition, from Figure 7, we notice that cell viability is further lowered with the use of folic acid when compared with all the other formulations in all the drug concentration cases. This situation was also repeated at all treatment times. As the concentration of the drugs is the same, the lower viability of cells implies that the result could be due to the targeting effect of folic acid. As there was a propensity for NPs conjugated with folic acid to accumulate within cancer cells, a higher concentration of the drug would be present leading to higher cell mortality. The results also act in coordination with those shown in the cellular uptake test.

Quantitative analysis of the dosage form for *in vitro* therapeutic effect was carried out from the *in vitro* cell viability data. The IC₅₀, which is an *in vitro* therapeutic index defined as the drug concentration needed to kill 50% of the incubated cells in a designated time period, was calculated from the evaluation (Table 2). The IC₅₀ value after 24-h treatment is 0.026 μg/ml for T2k NP and 0.0025 μg/ml for T2k NP-FOL. The results demonstrated that the folic acid-conjugated NP formulation could be 90.4% more effective than the same NPs of no folic acid conjugation. Particularly, this is just a preliminary proof-of-concept *in vitro* experimental results, which should be further confirmed by the *in vivo* experiments.

Conclusions

A series of long-chain TPGS_{nk} surfactants, that is TPGS2k, TPGS5k, and TPGS2kNH₂, were successfully syn-

thesized in this study. Docetaxel-loaded PLGA NPs were prepared using the nanoprecipitation method with those surfactants used in the emulsification process. The long-chain-coated PLGA NPs were characterized and their *in vitro* performance was evaluated. Folic acid was conjugated onto TPGS2kNH₂-coated PLGA NPs for targeted chemotherapy. Comparison of the characteristics between the PLGA NPs prepared with the various long-chain surfactants and the bare PLGA NPs showed similar characteristics in terms of size, size distribution, and surface morphology. However, the former were shown to have significantly higher drug loading, greater cellular uptake efficiency and cytotoxicity than the latter *in vitro*. The folic acid conjugation on the NPs further increased the cellular uptake efficiency and cytotoxicity. The long-chain surfactant TPGS2k seems to have the best effects in NP formulation of anticancer drugs among the various TPGS_{nk} surfactants. Folic acid conjugation can further promote the targeted drug delivery to the cancer cells of folate overexpression.

Acknowledgments

This work is supported by the Singapore–China Collaborative Grant, A*STAR, Singapore (PI: Feng S.-S.). The authors thank Mr. Jonathan Siow Yong Fatt, a FYP student in the ChBE Department for his contribution in experiment. Y. T. Liu is grateful to the National University of Singapore for his PhD scholarship. The authors also appreciate Dr. Y. C. Dong for inspiring discussion, Dr. K. Li, Dr. Z. L. Yuan, and Ms. S. Y. Lee for their technical assistance in experiments.

Literature Cited

- Jemal A, Siegel R, Ward E, Hao Y, Xu J, Thun MJ. Cancer statistics, 2009. *CA Cancer J Clin*. 2009;59:225–249.
- Jemal A, Siegel R, Xu J, Ward E. Cancer statistics, 2010. *CA Cancer J Clin*. 2010;60:277–300.
- Feng SS. New-concept chemotherapy by nanoparticles of biodegradable polymers: where are we now? *Nanomedicine (UK)*. 2006;1:297–309.
- Feng SS, Chien S. Chemotherapeutic engineering: application and further development of chemical engineering principles for chemotherapy of cancer and other diseases. *Chem Eng Sci*. 2003;58:4087–4114.
- Ferrari M. Cancer nanotechnology: opportunities and challenges. *Nat Rev Cancer*. 2005;5:161–171.
- Farokhzad OC, Langer R. Impact of nanotechnology on drug delivery. *ACS Nano*. 2009;3:16–20.
- Sinha R, Kim GJ, Nie S, Shin DM. Nanotechnology in cancer therapeutics: bioconjugated nanoparticles for drug delivery. *Mol Cancer Ther*. 2006;5:1909–1917.
- Feng SS, Zhao L, Zhang Z, Bhakta G, Win KY, Dong Y, Chien S. Chemotherapeutic engineering: vitamin E TPGS-emulsified nanoparticles of biodegradable polymers realized sustainable paclitaxel chemotherapy for 168 h *in vivo*. *Chem Eng Sci*. 2007;62:6641–6648.
- Gan CW, Chien S, Feng SS. Enhancement of chemotherapeutic efficacy of docetaxel by using a biodegradable nanoparticle formulation. *Curr Pharm Design*. 2010;16:2308–2320.
- Zhang L, Gu FX, Chan JM, Wang AZ, Robert L, Farokhzad OC. Nanoparticles in medicine: therapeutic applications and developments. *Clin Pharmacol Ther*. 2008;83:761–769.
- Cho K, Wang X, Nie S, Chen ZG, Shin DM. Therapeutic nanoparticles for drug delivery in cancer. *Clin Cancer Res*. 2008;14:1310–1316.
- Tong R, Cheng J. Anticancer polymeric nanomedicines. *Polym Rev*. 2007;47:3450–3481.
- Feng SS. Nanoparticles of biodegradable polymers for new-concept chemotherapy. *Expert Rev Med Dev*. 2004;1:115–125.
- Nie S. Understanding and overcoming major barriers in cancer nanomedicine. *Nanomedicine (UK)*. 2010;5:523–528.
- Owens DE, Peppas NA. Opsonization, biodistribution, and pharmacokinetics of polymeric nanoparticles. *Int J Pharm*. 2006;307:93–102.
- Jain RK. Physiological barriers to delivery of monoclonal antibodies and other macromolecules in tumors. *Cancer Res*. 1990;50:814–819.

17. Minchinton AI, Tannock IF. Drug penetration in solid tumours. *Nat Rev Cancer*. 2006;6:583–592.
18. Dreher MR, Liu W, Micheli CR, Dewhirst MW, Yuan F, Chilkoti A. Tumor vascular permeability, accumulation, and penetration of macromolecular drug carriers. *J Natl Cancer Inst*. 2006;98:335–344.
19. Sadoqi M, Lau-Cam CA, Wu SH. Investigation of the micellar properties of the tocopheryl polyethylene glycol succinate surfactants TPGS 400 and TPGS 1000 by steady state fluorometry. *J Colloid Interface Sci*. 2009;333:585–589.
20. Win KY, Feng SS. In vitro and in vivo studies on vitamin E TPGS-emulsified poly(D,L-lactic-co-glycolic acid) nanoparticles for paclitaxel formulation. *Biomaterials*. 2006;27:2285–2291.
21. Gao Y, Li LB, Zhai G. Preparation and characterization of pluronic/TPGS mixed micelles for solubilization of camptothecin. *Colloid Surface B*. 2009;64:194–199.
22. Mu L, Seow PH. Application of TPGS in polymeric nanoparticulate drug delivery system. *Colloid Surface B*. 2006;47:90–97.
23. Feng SS, Mei L, Anitha P, Gan CW, Zhou W. Poly(lactide)-vitamin E derivative/montmorillonite nanoparticle formulations for the oral delivery of docetaxel. *Biomaterials*. 2009;30:3297–3306.
24. Mu L, Feng SS. Vitamin E TPGS used as emulsifier in the solvent evaporation/extraction technique for fabrication of polymeric nanospheres for controlled release of paclitaxel (Taxol). *J Control Release*. 2002;80:129–144.
25. Dintaman JM, Silverman JA. Inhibition of P-glycoprotein by D- α -tocopheryl polyethylene glycol 1000 succinate (TPGS). *Pharm Res*. 1999;16:1550–1556.
26. Shidhaye S, Lotlikar V, Malke S, Kadam V. Nanogel engineered polymeric micelles for drug delivery. *Curr Drug Ther*. 2008;3:209–217.
27. Li SD, Huang L. Nanoparticles evading the reticuloendothelial system: Role of the supported bilayer. *Biochim Biophys Acta*. 2009;1788:2259–2266.
28. Gaur U, Sahoo SK, De TK, Ghosh PC, Maitra A, Ghosh PK. Bio-distribution of fluoresceinated dextran using novel nanoparticles evading reticuloendothelial system. *Int J Pharm*. 2000;202:1–10.
29. Kah JCY, Wong KY, Neoh KG, Song JH, Fu JW, Mhaisalkar S, Olive M, Sheppard CJ. Critical parameters in the pegylation of gold nanoshells for biomedical applications: an in vitro macrophage study. *J Drug Target*. 2009;17:181–193.
30. Collnot EM, Baldes C, Wempe MF, Hyatt J, Navarro L, Edgar KJ, Schaefer UF, Lehr CM. Influence of vitamin E TPGS poly(ethylene glycol) chain length on apical efflux transporters in Caco-2 cell monolayers. *J Control Release*. 2006;111:35–40.
31. Engels FK, Mathot RA, Verweij J. Alternative drug formulations of docetaxel: a review. *Anti-Cancer Drugs*. 2007;18:95–103.
32. Bilati U, Allemann E, Doelker E. Development of a nanoprecipitation method intended for the entrapment of hydrophilic drugs into nanoparticles. *Eur J Pharm Sci*. 2005;24:67–75.
33. Win KY, Feng SS. Effects of particle size and surface coating on cellular uptake of polymeric nanoparticles for oral delivery of anti-cancer drugs. *Biomaterials*. 2005;26:2713–2722.
34. Decuzzi P, Ferrari M. The role of specific and non-specific interactions in receptor-mediated endocytosis of nanoparticles. *Biomaterials*. 2007;28:2915–2922.
35. Yoo HS, Park TG. Folate receptor targeted biodegradable polymeric doxorubicin micelles. *J Control Release*. 2004;96:273–283.

Manuscript received Aug. 19, 2011, and revision received Oct. 25, 2011.